

Prepared for X-ray  
Symposium, Univ.  
of Denver, July 1963  
Dewey U. 3 Aug 7-9

N45-88885  
~~163-16361~~

AN EXPLANATION OF MICROSTRUCTURES IN THE  
TANTALUM-CARBON SYSTEM

By G. Santoro and H. B. Probst

Lewis Research Center  
National Aeronautics and Space Administration  
Cleveland, Ohio

INTRODUCTION

Considerable interest has developed in recent years in the tantalum-carbon system. This interest stems primarily from the melting temperatures reported for the compound TaC. This carbide melts as high as 3800° to 3900° C (refs. 1 to 3) and is, therefore, one of the highest melting materials known.

Ellinger (ref. 4) published the results of his work on the Ta-C system in 1943. His phase diagram showed two carbides, Ta<sub>2</sub>C, a hexagonal structure, and TaC, a NaCl structure. After carburizing a Ta rod, Ellinger observed a microstructure showing a very definite carbon gradient with concentric bands, each containing two phases, in which the second (minor) phase always existed as apparently straight platelets. Rhines, in the discussion to Ellinger's paper, correctly pointed out that these two-phase regions in binary diffusion couples were simply the result of precipitation occurring on cooling as a result of solubility limits decreasing with temperature.

Since Ellinger's paper, details of the phase diagram have been refined, but the basic qualitative equilibrium relationships are unchanged. An accepted diagram compiled from the results of many investigations is shown in figure 1 (ref. 5). More recently, studies

~~Available to NASA Offices and  
NASA Centers Only.~~

E-2207

in the Ta-C system (refs. 6 to 9) have observed microstructures similar to those of Ellinger, but, in many cases, the possibility of these structures being the result of precipitation seems to have been ignored. The characteristic straight platelet structures have been variously described as "twins," "striated structure," and "structure of unknown origin."

It is the purpose of this paper to show these structures to be the result of precipitation processes and to account for their characteristic appearance by a precipitation model based on the geometries of the crystal structures involved.

#### EXPERIMENTAL PROCEDURE

The Ta-C compositions for this study were made by carburizing 0.010-in. high-purity Ta wires in a purified hydrocarbon gas (toluene or propane). The Ta wire was heated by its own electrical resistance, and the overall carbon content of the resulting structure was controlled by hydrocarbon gas pressure. A detailed account of this method is given in reference 9. The structures studied were produced by heating for 6 hr at 1800° C followed by rapid cooling unless otherwise specified. Carburized filaments were homogeneous in cross section only if their carbon content placed them well into a single-phase field. Filaments whose overall carbon contents were near the solubility limits of single phases or within a two-phase field were heterogeneous with strongly developed annular structures, i.e., concentric rings. The carbon content reported for any one filament exhibiting an annular structure is an overall composition, and it should

be remembered that the case will be of higher carbon content while the core will be lower than the average carbon concentration. The average carbon concentrations were determined by a combustion method and refer to total carbon. The small quantity of sample precluded reliable free-carbon analysis. It is believed, however, that the amount of free carbon is negligible, since no evidence of free carbon was found in the metallographic examinations or the X-ray patterns.

Phase identification was accomplished by standard X-ray diffraction techniques. Diffraction patterns were obtained from as-reacted filament surfaces, powdered filaments, and remaining ductile (unpowderable) cores when these were present. In this manner, phase identification by diffraction was correlated to microstructure.

Metallographic sections of the filaments were prepared by standard mounting and polishing techniques. After investigating several etches, one consisting of 3/1  $\text{HNO}_3/\text{HF}$  was found to give the most consistent results. This etch was used for all samples of this study.

Microhardness measurements were made with a 135° diamond pyramid and a 50 g load. This load was determined as the best to give good readings over the wide range of hardnesses from TaC to soft Ta.

#### MODEL

Before examining the actual structures obtained, let us consider a model of precipitation based upon the crystallographic structures involved. Consider the precipitation of  $\beta$  from  $\gamma$  as the solu-

bility limit for Ta is exceeded during cooling. The matrix  $\gamma$  is a NaCl structure with a lattice parameter at the solubility limit of 4.4104 Å (ref. 10). The arrangement of a unit cell of this structure is shown in figure 2 (not taking into account vacant carbon sites). Any {111} plane of this structure may be considered to consist entirely of C or Ta atoms in a hexagonal arrangement with a spacing of 3.12 Å between nearest neighbors.

The  $\beta$  phase, which must precipitate from  $\gamma$ , has a hexagonal structure and must be saturated in C. The lattice parameters for this  $\beta$  are  $a_0 = 3.104$  Å and  $c_0 = 4.942$  Å, and a unit cell is shown in figure 3. The basal plane of this structure consists of a hexagonal arrangement of Ta (or C) atoms with a nearest-neighbor spacing of 3.104 Å.

Comparing the {111} plane of  $\gamma$  and the basal plane of  $\beta$  shows that both have identical geometries with a linear mis-match of only about 0.5%; thus a very favorable situation exists for  $\beta$  to precipitate on {111} planes of  $\gamma$  on cooling. The same geometrical situation exists if  $\gamma$  precipitates from  $\beta$ . The same compositions and therefore lattice parameters must be considered, and it is therefore seen that  $\gamma$  precipitation on the basal plane of  $\beta$  is also highly probable.

Precipitation reactions with such lattice relationships have been observed in metal systems. For example, hexagonal  $\text{AgAl}_2$  precipitates from Ag saturated face-centered cubic Al solid solution so that the {0001} plane of  $\text{AgAl}_2$  is parallel to the {111} plane of the

Al solution (ref. 11). An example of a cubic precipitate from a hexagonal matrix is found in the Mg-Sn system (ref. 12). In this case the simple cubic ( $\text{CaF}_2$  structure)  $\text{Mg}_2\text{Sn}$  precipitates with its  $\{111\}$  plane parallel to the  $\{0001\}$  plane of the Mg solid-solution matrix. Although the habit plane and direction in the  $\text{Mg}_2\text{Sn}$  precipitate can be varied by heat treatment, the precipitate is always rejected from solution on the basal plane of the matrix.

In the case of TaC-Ta<sub>2</sub>C precipitation, it is not assumed here that there is necessarily a coherency between matrix and precipitate but only that the plane of the matrix on which precipitation occurs is the close-packed plane (i.e.,  $\{111\}$  for the cubic TaC matrix and  $\{0001\}$  for the hexagonal Ta<sub>2</sub>C matrix). The high degree of matching between these planes does suggest, however, that coherent precipitation is a very distinct possibility.

If the close-packed planes are the precipitation planes as assumed here, then the precipitation of either carbide from the other should result in a Widmanstätten structure - there should be characteristic differences, however, depending on which carbide is the matrix. In the precipitation of  $\beta$  from  $\gamma$ , the  $\{111\}$  plane of  $\gamma$  actually provides four potential precipitation planes, since in the cubic geometry there are four  $\{111\}$  planes. Therefore in a single grain of  $\gamma$ , platelets of  $\beta$  precipitate might be expected in up to four directions. Conversely, when  $\gamma$  precipitates from  $\beta$ , the singular basal plane of the hexagonal symmetry provides but one precipitation plane. Hence, in a single grain of  $\beta$  the platelets of  $\gamma$  precipitate should be found in only one direction.

### EXPERIMENTAL RESULTS

Numerous microstructures in the Ta-C system were examined. Representative structures will be discussed here proceeding from high carbon compositions to low carbon.

#### TaC<sub>0.88</sub>

Figure 4 shows the structure corresponding to a composition of TaC<sub>0.88</sub> well within the  $\gamma$  single-phase field. The structure shows a single-phase material and is representative of all compositions between TaC<sub>0.74</sub> and TaC<sub>0.98</sub>. X-ray analysis of such a structure gives only the TaC pattern, and the hardness of this particular composition is DPH 2700.

#### TaC<sub>0.64</sub>

The structure obtained at a composition of TaC<sub>0.64</sub> is shown in figure 5. The characteristic annular structure is apparent. X-ray analysis of this material shows the presence of both  $\gamma$  and  $\beta$ <sup>1</sup>. Such a two-phase structure is characteristic of compositions between TaC<sub>0.52</sub> and TaC<sub>0.74</sub>. Slow cooling of samples within this composition range gave identical structures, thus ruling out the possibility of these structures being the result of metastable transformations. Within this range as lower carbon concentrations are approached, the  $\beta$  phase becomes more evident in the X-ray patterns, the inner structure (core) occupies a larger portion of the cross section, and a small central core of single-phase  $\beta$  becomes evident. The hardness

---

<sup>1</sup>Some lines corresponding to those reported by Lesser and Brauer (ref. 13) as belonging to an unknown  $\xi$  phase were observed for some compositions between TaC<sub>0.4</sub> and TaC<sub>0.6</sub>. The origin and significance of this phase is not known at the present time.

of the two zones shown in figure 5 are DPH 1620 and DPH 1520 for the case and core, respectively. This hardness for the core represents an increase over that of single-phase  $\beta$  (DPH  $\approx$  1000), while the value for the case seems to be essentially the same as carbon deficient  $\gamma$  (DPH  $\approx$  1600 (ref. 9)).

The appearance of this structure and the results of X-ray diffraction ( $\gamma$  and  $\beta$  present) give support to the proposed precipitation model. During the carburizing treatment, a carbon deficient  $\gamma$  of the case was in equilibrium with the carbon saturated  $\beta$  core. Upon cooling solubility limits were exceeded with  $\beta$  precipitating from  $\gamma$  in the case and  $\gamma$  precipitating from  $\beta$  in the core according to the proposed lattice relationship. The multidirectional platelets of  $\beta$  are evident in the case, while the core exhibits unidirectional  $\gamma$  platelets within any one  $\beta$  grain. The increasing size of the core with decreasing carbon and the eventual stabilization of a small single-phase  $\beta$  core are in accord with the equilibrium diagram shown in figure 1 and with the proposed explanation of the microstructures. Another observation in support of the precipitation model is the fact that in all carburized samples exhibiting both unidirectional and multidirectional structures the region containing the multidirectional platelets is always located nearer the sample surface than the unidirectional structure. This is in accord with the carbon gradient that exists at the carburizing temperature; i.e., the  $\gamma$  phase from which  $\beta$  precipitates being of higher carbon content is located nearer the surface than the  $\beta$  from which  $\gamma$  precipitates; thus the  $\gamma$  matrix with multidirectional  $\beta$  precipitate always is found nearer the sample surface than the lower carbon  $\beta$  matrix containing unidirectional  $\gamma$  precipitate.

The constant solubility of carbon in  $\beta$  as a function of temperature as indicated in figure 1 must be in error, since the observed precipitation of  $\gamma$  from  $\beta$  is indicative of decreasing carbon solubility in  $\beta$  with decreasing temperature. Similar structures have been found in work with the Nb-C system; however, no such structures were observed in the Hf-C system (ref. 7). This again supports the precipitation explanation proposed here, since these observations are obviously due to the similarity between the Ta-C and Nb-C equilibrium relationships (both exhibiting a dimetal carbide), while in the Hf-C system an equilibrium dimetal carbide does not exist.

The hardness values for the structures shown in figure 5 suggest that the presence of a hard  $\gamma$  precipitate in a relatively soft  $\beta$  matrix (the core) increases the hardness over that of the  $\beta$  matrix (DPH = 1000), while conversely, the presence of  $\beta$  precipitate in the very hard  $\gamma$  matrix shows little effect on the hardness as compared to that on the hardness of single-phase carbon deficient  $\gamma$  (DPH  $\approx$  1600, ref. 9).

#### TaC<sub>0.31</sub>

A typical structure resulting at low carbon concentrations is shown in figure 6. At the composition of TaC<sub>0.31</sub>, figure 1 shows the equilibrium phases to be  $\alpha$  and  $\beta$ <sup>2</sup>. X-ray analysis of the surface of the as-reacted sample gave only the  $\beta$  pattern, while analysis of the core alone (after removing the brittle case) gave both  $\beta$  and  $\alpha$ .

---

<sup>2</sup>Samples consisting of only single-phase  $\beta$  are difficult to make by the carburization method owing to the limited composition range of the phase at low temperatures.



The hardness of the case is DPH 860 possibly representing a slight decrease of hardness for carbon deficient  $\beta$  as compared to DPH 1000 for carbon saturated  $\beta$ . This is in agreement with reference 14, which gives hardness values of 810 and 947 for carbon deficient and carbon saturated  $\beta$ , respectively. The core has a hardness of DPH 120, this along with X-ray results and appearance suggests a random precipitation of  $\beta$  in  $\alpha$ . Structures similar to that of figure 6 were obtained at all compositions below about  $\text{TaC}_{0.43}$  with the  $\alpha$  matrix core occupying a larger portion of the cross section as the carbon concentration is decreased. At compositions above  $\text{TaC}_{0.43}$ , near  $\beta$ , the entire cross section appeared as the case in figure 6. While X-ray analysis showed only  $\beta$  for such structures, the dark apparently lamellar regions appear to be a second phase and warranted further investigation.

This lamellar structure is of particular interest, since Ellinger (ref. 4) observed similar but somewhat better developed structures in his low carbon sample and Rhines in the discussion of Ellinger's paper suggested these might be the result of a low-temperature eutectoid decomposition of  $\beta$  to  $\alpha$  plus  $\gamma$ . With this in mind, a sample was prepared at a composition of  $\text{TaC}_{0.36}$  and slowly cooled from the reaction temperature (a period of  $1\frac{1}{4}$  hr to cool to  $\approx 800^\circ \text{C}$ ) in order to allow full development of a eutectoid structure if it exists. The resulting structure is shown in figure 7. A lamellar structure in the case (which was  $\beta$  at the reaction temperature) was indeed developed; however, X-ray patterns from the surface of

this sample showed the presence of  $\alpha$  plus  $\beta$  and not  $\alpha$  plus  $\gamma$ . This then indicates that eutectoid decomposition of  $\beta$  does not occur; however, a lamellar structure was developed by this treatment and must be explained. Since the two phases present as indicated by X-ray are  $\beta$  and  $\alpha$ , it would appear that this structure represents a precipitate of  $\alpha$  in a  $\beta$  matrix. The difference between this well-developed lamellar structure and that of figure 6 must be due to a slow cooling rate which leads to a more complete precipitation and the elimination of a nonequilibrium supersaturated solid solution that results by quenching.

The hardness of the two-phase  $\alpha$  plus  $\beta$  case is 770, while that of the core is 120. These compare well with the hardnesses of the rapidly cooled structure of figure 6 showing a slight decrease in the hardness of the case due to the presence of the soft  $\alpha$  precipitate.

The unidirectional nature of the  $\alpha$  precipitate in  $\beta$  is interesting. Comparing the two close-packed planes of the two phases shows the  $\{110\}$  plane of carbon saturated  $\alpha$  to be a distorted hexagonal arrangement with nearest-neighbor spacings of 2.865 and 3.305 Å and included angles within the unit triangle to be 54.7, 54.7, and 70.6° (calculated from  $a_0$  of Ta = 3.305 Å (ref. 13)). This compares to the true hexagonal arrangement in the  $\{0001\}$  plane of Ta saturated  $\beta$  in which the nearest-neighbor spacing is 3.101 Å and of course the included angles are all 60°. This comparison yields an average mismatch of about 2.7% for placing one unit triangle upon the other; this misfit increases, however, as the precipitate grows.

The fact that  $\alpha$  seems to precipitate from  $\beta$  in a Widmanstätten structure but yet the  $\beta$  precipitation from  $\alpha$  appears to be the random (see the core of fig. 6) may be due to the increasing misfit with size of precipitate. In the case where lamellar structure form, the metallic bonding of the  $\alpha$  phase may allow it to readily distort to accommodate the increasing misfit and thus grow as a continuous platelet. On the other hand, the hybrid metallic-covalent bonding of the  $\beta$  phase does not allow such distortion; thus as the  $\beta$  precipitate grows, it may lose coherency with the  $\alpha$  matrix and result in random precipitation.

#### CONCLUSIONS

As a result of this investigation, the following conclusions may be drawn:

1. The characteristic striated (Widmanstätten) structures found in the Ta-C system at compositions between  $Ta_2C$  and TaC are the result of precipitation reactions in which the close-packed plane of each phase is the plane of precipitation.
2. The maximum solubility of C in  $Ta_2C$  must decrease with decreasing temperature rather than remain constant as the presently accepted phase diagram indicates.
3. There is no evidence for a eutectoid decomposition of  $Ta_2C$ .
4. Tantalum can precipitate from  $Ta_2C$  giving a unidirectional Widmanstätten structure; however,  $Ta_2C$  precipitation from tantalum is random apparently because of the inability of  $Ta_2C$  to distort and maintain coherency with the tantalum matrix.

REFERENCES

1. Friederich, E., and Sittig, L., Z. Anorg. Allg. Chem., V. 144, p. 174 (1925).
2. Agte, C., and Alterthum, H., Z. Tech. Physik, V. 11, p. 182 (1930).
3. Zalabak, C. F., NASA TN D-761, Mar. 1961.
4. Ellinger, F. H., Trans. A.S.M., V. 31, p. 89 (1943).
5. Storms, E. K., LAMS-2674 Part 1. Feb. 1, 1962.
6. Dolloff, R. T., Progress Report No. 1. National Carbon Co., Contract AF 33(657)-8025, June 10, 1962.
7. High Temperature Materials, Inc. Final Report. Contract N0w60-0292, Sept. 30, 1961.
8. Vargo, E. J., Thompson Ramo Wooldridge, Inc. TM-1575-CM, June 29, 1960.
9. Santoro, G., To be published by A.I.M.E.
10. Bowman, A. L., Jour. Phys. Chem., V. 65, p. 1596 (1961).
11. Mehl, R. F., and Barrett, C. S., A.I.M.E. Trans., V. 93, p. 78 (1931).
12. Derge, G., Kommel, A. R., and Mehl, R. F., A.I.M.E. Trans., V. 124, p. 367 (1937).
13. Lesser, R., and Brauer, G., Z. für Metallkunde, V. 49, p. 622 (1958).
14. Samsonov, G. V., and Rukina, V. B., Dopovidi Akad. Nauk. Ukr. RSR., no. 3, p. 247 (1957).

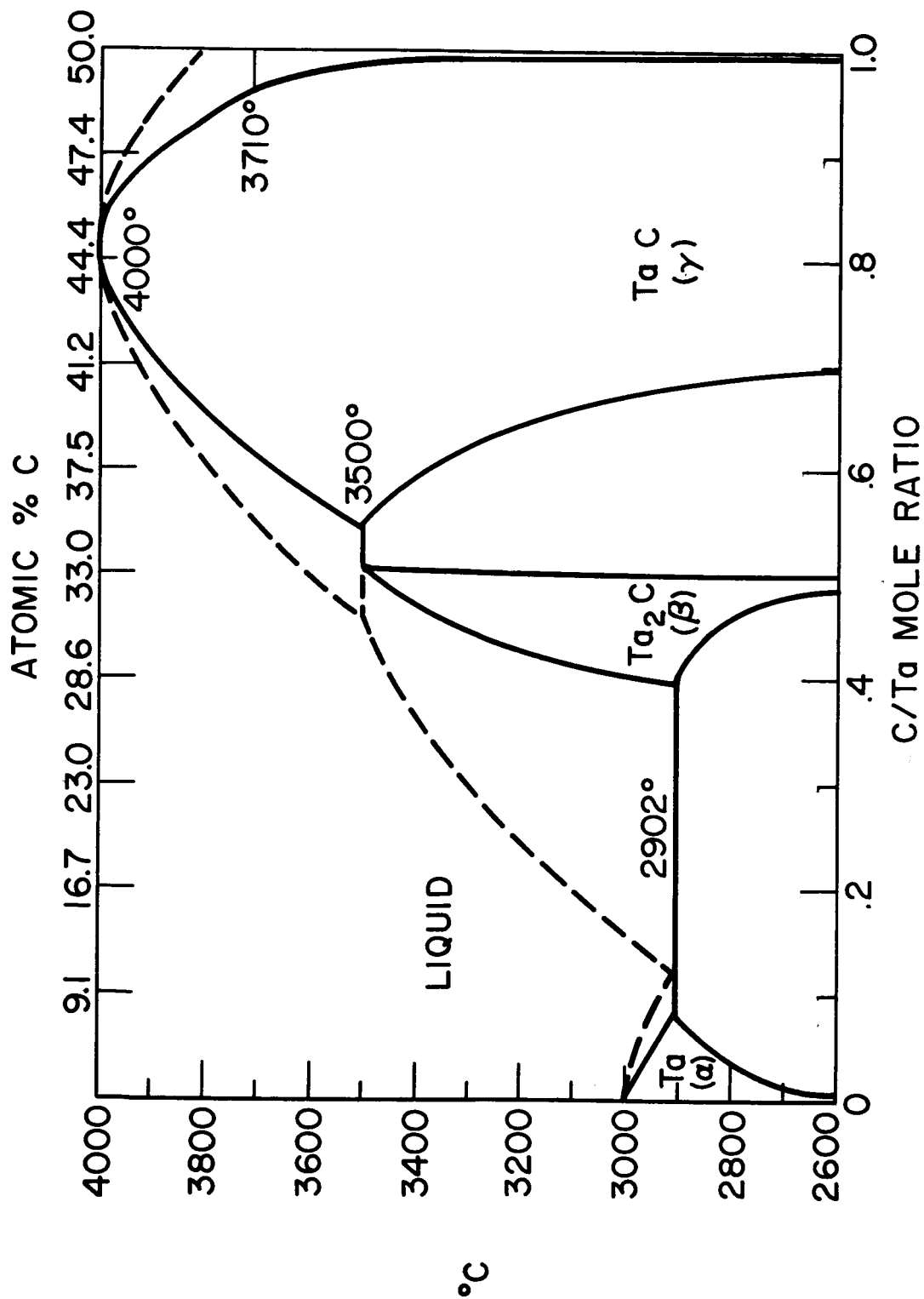


Figure 1. - Phase diagram of the Ta-TaC system (Ref. 5).

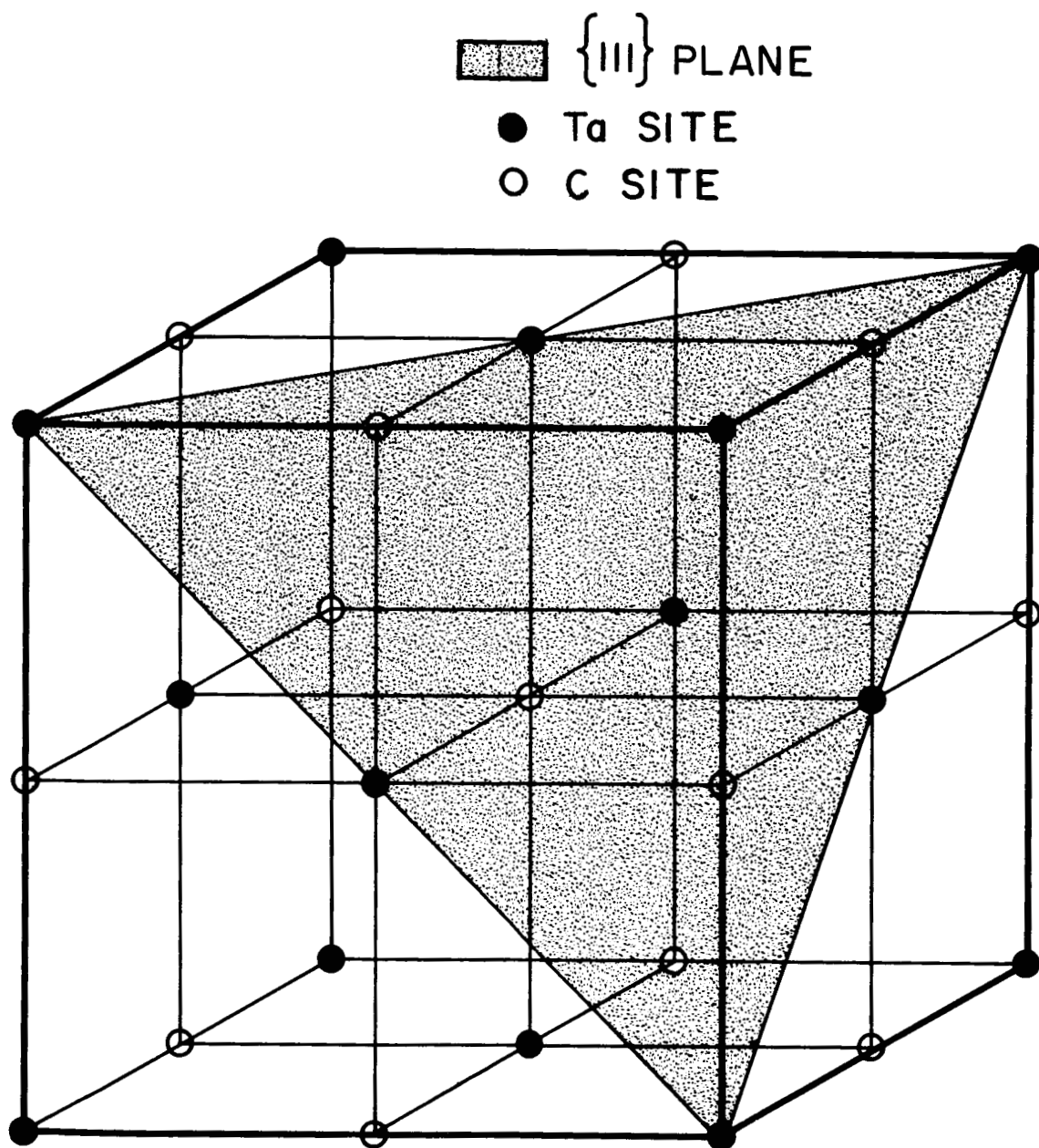


Figure 2. -  $\gamma$  (TaC) Unit Cell.

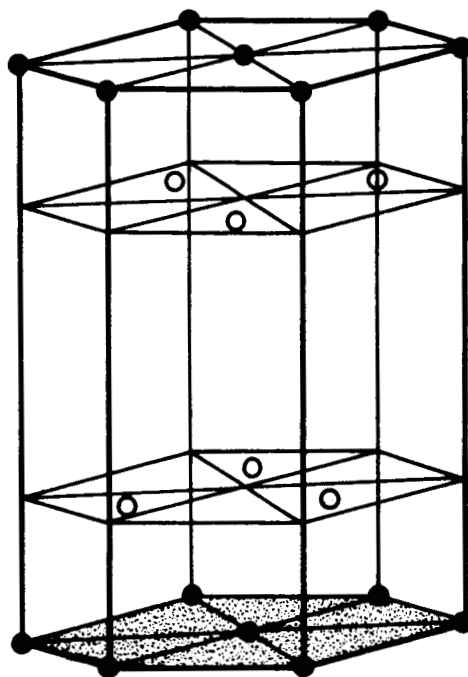
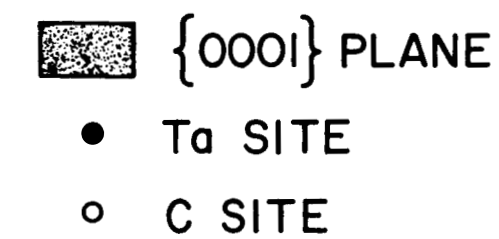


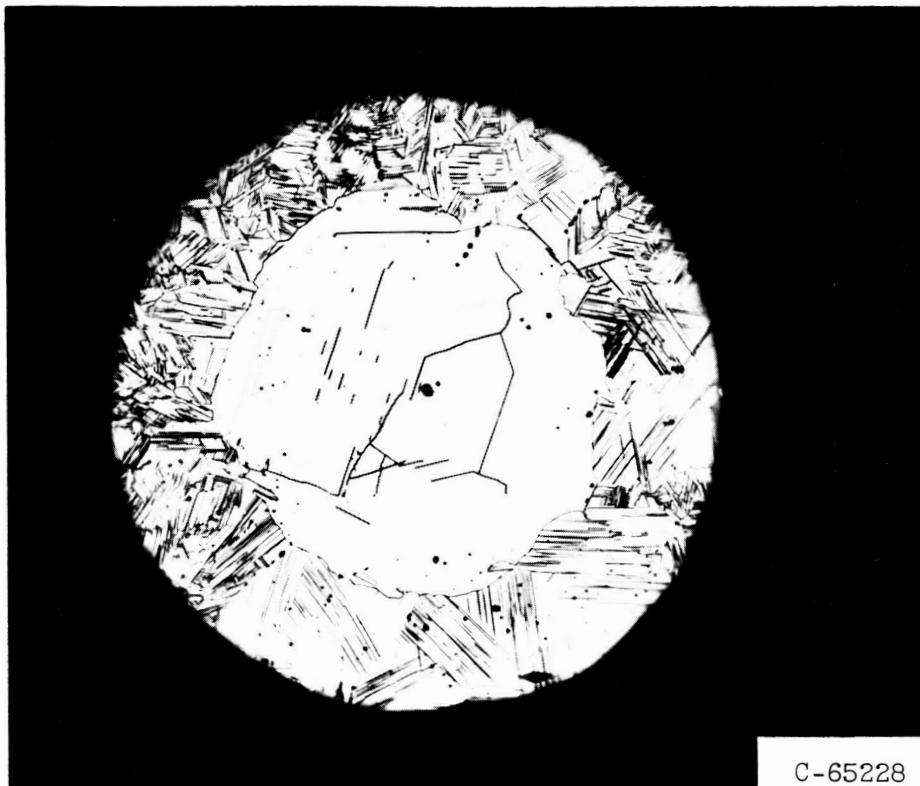
Figure 3. -  $\beta$  ( $\text{Ta}_2\text{C}$ ) Unit Cell.



C-65227

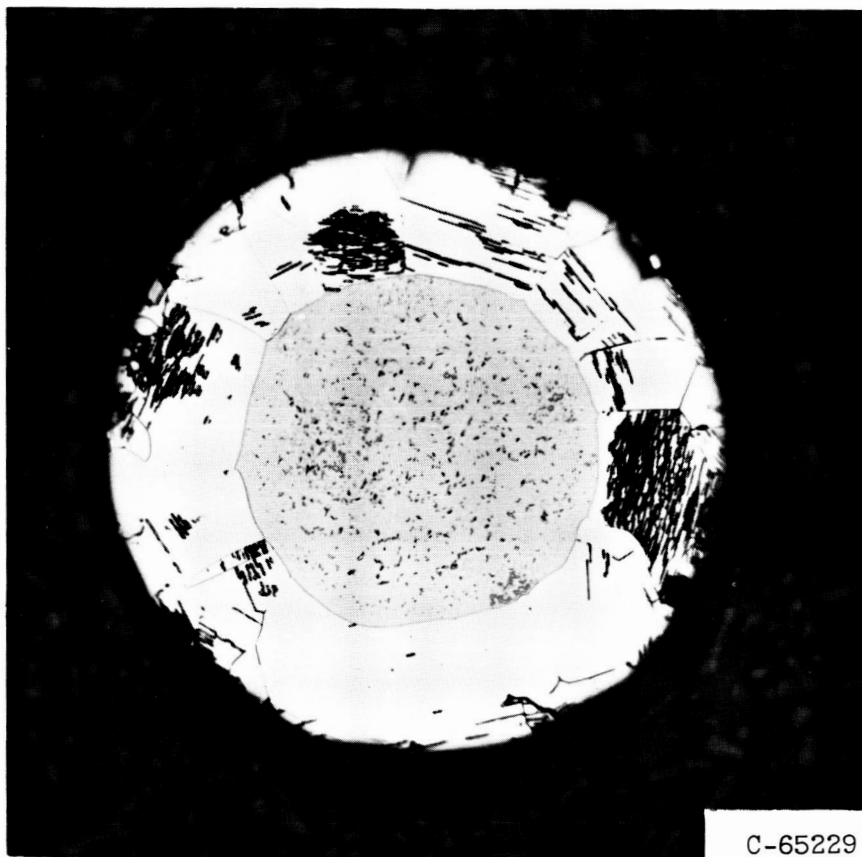
Figure 4. - Microstructure of TaC.<sub>88</sub>; etchant, 3HNO<sub>3</sub>/HF;  
×300. DPH = 2700.





C-65228

Figure 5. - Microstructure of TaC.<sub>64</sub>; etchant,  $3\text{HNO}_3/\text{HF}$ ;  $\times 300$ . DPH case = 1620, DPH core = 1520.



C-65229

Figure 6. - Microstructure of TaC.<sub>31</sub>; etchant,  $3\text{HNO}_3/\text{HF}$ ;  
x300. DPH case = 860, DPH core = 120.



C-65230

Figure 7. - Microstructure of TaC<sub>.36</sub>;  
slow cool - etchant,  $3\text{HNO}_3/\text{HF}$ ;  $\times 300$ .  
DPH case = 770, DPH core = 120.